Catalytic Hydrodeoxygenation of Guaiacol on Rh-Based and Sulfided CoMo and NiMo Catalysts

ARTICLE *in* ENERGY & FUELS · FEBRUARY 2011

Impact Factor: 2.79 · DOI: 10.1021/ef101521z

5 AUTHORS, INCLUDING:

Yu-Chuan Lin
National Cheng Kung University
37 PUBLICATIONS **994** CITATIONS
SEE PROFILE

Hou-Peng Wan
Industrial Technology Research Institute
23 PUBLICATIONS **244** CITATIONS
SEE PROFILE

energy&fuels

ARTICLE

pubs.acs.org/EF

Catalytic Hydrodeoxygenation of Guaiacol on Rh-Based and Sulfided CoMo and NiMo Catalysts

Yu-Chuan Lin,*[,†] Chia-Liang Li,[†] Hou-Peng Wan,[‡] Hom-Ti Lee,[‡] and Chiung-Fang Liu[‡]

[†]Department of Chemical Engineering and Materials Science, Yuan Ze Fuel Cell Center, Yuan Ze University, Chungli, Taiwan 32003

[‡]Green Energy and Environment Research Laboratories, Industrial Technology Research Institute, Hsinchu, Taiwan 31040

ABSTRACT: This study investigates the hydrodeoxygenation (HDO) of guaiacol (GUA), a lignin model compound, using two types of catalysts: mono- and bimetallic Rh-based catalysts and classical sulfided CoMo and NiMo catalysts. The former exhibited greater reactivity than the latter. However, substituting some of the Rh ions with another noble metal (i.e., Pd or Pt) produced no positive effect. This study also proposed the mechanisms of GUA HDO for both types of catalysts. The first step of Rh-based catalysts was hydrogenation of GUA's benzene ring, followed by demethoxylation and dehydroxylation. As for the sulfided CoMo and NiMo catalysts, GUA HDO began with demethylation, demethoxylation, and deoxygenation, followed by benzene ring saturation. A better understanding of HDO surface chemistry may lead to more efficient catalysts for target products.

1. INTRODUCTION

Lignin is the most abundant polymer containing organic aromatics in the plant kingdom.[1,2] However, it has traditionally been viewed as a waste byproduct or used as a low-grade fuel.[2−4] This is primarily due to the difficulty of converting lignin to high-grade fuels and chemicals.[2,5] Yet, advanced developments of agriculture and biology in lignocellulosic biomass breeding,[6] together with declining crude oil reserves and worldwide environmental concerns have recently drawn unprecedented attention to lignin conversion.[7,8]

Hydrodeoxygenation (HDO) is a promising method of lignin conversion. HDO is a process in which hydrogen acts as a reductant for deoxygenation, and is typically performed in a batch[9,10] or a continuous system[11,12] with catalysts. Oxygen can be removed in the form of water under H_2-pressured hydrothermal conditions.[13] As a result, the upgraded products contain less oxygen, providing them with a higher heating value and rendering them chemically more stable than in their unrefined state.[13]

Guaiacyl species are the primary structure in lignin.[2] A significant number of guaiacyl groups, including guaiacol (GUA, $C_7H_8O_2$), vanillin ($C_8H_8O_3$), and eugenol ($C_{10}H_{12}O_2$), can be produced through various conversion approaches such as pyrolysis[14,15] and liquefaction.[5,16] This leads guaiacyl species to be a common representative of lignin and its derivatives.[10,17−19] An effective upgrading process for guaiacyl species should facilitate the design of a lignin conversion platform.

The most common HDO catalysts are sulfided CoMo and NiMo on Al_2O_3. In 1970, a Canadian patent filed by Alpert and Shuman[20] revealed the potential of lignin conversion using CoMo catalysts. This inspired follow-up GUA HDO studies. Hurff and Klein[21] employed sulfided CoMo/Al_2O_3 for the HDO of anisole (C_7H_8O) and GUA, respectively, in an autoclave. By observing the product distribution as a function of time, they proposed that demethylation is the first step of HDO process. Interestingly, based on the higher consumption rate of GUA than anisole, they suggested that the ortho hydroxyl group in the GUA structure could speed up demethylation activity. This finding was confirmed by a research team at University of Toronto[22] and Bredenberg and co-workers.[23] Delmon and collaborators[24−28] extensively investigated sulfided CoMo and NiMo systems by varying the surface chemistry of catalysts. They incorporated potassium and platinum as modifiers and used silica[25] and activated carbon[26−28] to replace Al_2O_3 as supports. Their results indicate that it is possible to control the HDO chemistry with the appropriate catalyst design. For example, introducing surface oxygen species on activated carbon can generate unique active site-support interactions, resulting in promising reactivity and product selectivity.[27−29] More recently, the Geantet group[30,31] used sulfided CoMo/Al_2O_3 to investigate the coprocessing of straight run gas oil with bio-oil model compounds, including GUA, in a hydrotreating pilot plant. Their research shows that it may be possible to treat oxygenates and hydrocarbons simultaneously in HDO and hydrodesulfurizaton processes. They also proposed a detailed mechanism of GUA conversion.

A recently published review by Zakzeski and collaborators[5] summarizes GUA HDO. Table 4 in their paper shows that sulfided CoMo and NiMo supported on Al_2O_3 are mainly used at temperatures ranging from 500 to 700 K under pressures of about 3−7 MPa. The major products of these reactions are six-membered ring compounds such as benzene and phenol. Compared to sulfided CoMo and NiMo on Al_2O_3, however, relatively few studies have used noble metal based catalysts. Despite their high cost, noble metal catalysts possess several advantages over conventional sulfide catalysts: (1) high reactivity at moderate temperature, achieving an energy efficient HDO process, (2) no sulfur stripping, and (3) flexible catalyst design by tailoring the active phase and support.[10,32]

Received: November 10, 2010
Revised: December 24, 2010
Published: February 15, 2011

Centeno and co-workers[25] doped trace platinum (~0.5 wt %) on a CoMo sulfide catalyst to achieve the HDO of GUA-type molecules, and reported a significant improvement in reactivity. Elliot and Hart[10] studied the catalytic HDO of a bio-oil-like compound (a mixture of furfural, GUA, acetic acid, and water) with palladium or ruthenium on carbon extrudates. Different hydrogenation abilities result in diverse hydrodeoxygenation pathways of GUA. Gutierrez and collaborators[32] explored mono- and bimetallic noble metal catalysts (including Pt, Rh, Pd, and their combinations) in GUA HDO. The reactivity could be changed by varying the composition of the active phase. In general, Rh-containing catalysts achieved better performances than other noble metal catalysts.

This study investigates the HDO chemistry of lignin derivatives. GUA served as the lignin model compound. Two types of HDO catalysts, Rh-based catalysts (Rh, PtRh, and PdRh on ZrO_2) and sulfided CoMo and NiMo on Al_2O_3 were used in GUA HDO. Catalyst characterization and the catalytic HDO testing were conducted. Based on these outcomes, plausible mechanisms mediated by these catalysts were thereby proposed.

2. EXPERIMENTAL SECTION

2.1. Catalyst Preparation. All catalysts in this study were prepared by the incipient wetness method. ZrO_2 (Aldrich, 99.99%) served as the support for Rh, PtRh, and PdRh catalysts. The precursors used in this study included $Pt(NH_3)_2(NO_2)_2$ (Aldrich, 3.4 wt % in dilute ammonium hydroxide), $Rh(NO_3)_3$ (Aldrich, 10 wt % Rh in >5 wt % nitric acid), and $Pd(NO_3)_2$ (Aldrich, 99.95%). The Rh content in Rh/ZrO_2 was 1 wt %. For bimetallic catalysts, an equivalent amount of Pt and Rh or Pd and Rh was used to allow 1 wt % loading. After impregnation, the resulting powder was dried at 80 °C overnight followed by calcination at 400 °C for 3 h using a heating rate of 5 °C/min.

To synthesize CoMo supported on Al_2O_3 (Aldrich, 99%), alumina was calcined at 600 °C overnight prior to the impregnation. An appropriate amount of $(NH_4)_6Mo_7O_{24}\cdot 4H_2O$ (Alfa Aesar, 99%) was first impregnated on alumina, and then dried at 80 °C overnight and calcined at 400 °C for 3 h using a 5 °C/min heating rate. Subsequently, a designated amount of $Co(NO_3)_2\cdot 6H_2O$ (Alfa Aesar, 98%) was impregnated on the Mo-containing powder, and subjected to the same drying−calcination process described above. The $NiMo/Al_2O_3$ catalyst was made with the same synthesis process, but replacing the Co precursor with $Ni(NO_3)_2\cdot 6H_2O$ (Alfa Aesar, 98%). The composition of the CoMo or NiMo catalyst was approximately 15 wt % of MoO_3 with 3 wt % of CoO or NiO.

2.2. Catalyst Characterization. Surface area was measured by the Brunauer, Emmet, and Teller (BET) method, using an automated N_2 adsorption system (Micrometrics ASAP 2010). Powder X-ray diffraction (XRD) patterns were recorded using a Shimadzu Labx XRD-6000 with a Cu−Kα radiation source. For sulfided catalysts and sulfur-containing samples, elemental analysis was conducted by an elemental analyzer (Elementar vario EL cube) using combustion method at 1150 °C to estimate sulfur contents. H_2-temperature programmed reduction (TPR) and temperature programmed desorption (TPD) of GUA were performed using the same instrumentation described previously.[33] This system consisted of a U-shaped cell and a temperature-controlled furnace. Approximately 0.1 g of sample was used for TPR trials. H_2 consumption was monitored by a thermal conductivity detector (TCD) in a 10% H_2/Ar stream. Approximately 0.1 g of CoMo or $NiMo/Al_2O_3$ was consumed in GUA TPD. About 0.2 g of Rh-based catalysts was required to produce sufficient signal-to-noise TCD signals. The catalyst was initially reduced at 300 °C for an hour at a 5 °C/min heating rate. After cooling to ambient temperature, GUA was introduced into the cell overnight through a saturator with an Ar stream (30 mL/min) as the carrier gas. The sample was subsequently purged with a He stream (30 mL/min) at 220 °C for 1 h to remove physisorbed GUA. After attaining a stable TCD baseline, TPD was performed from 220 to 700 °C (5 °C/min).

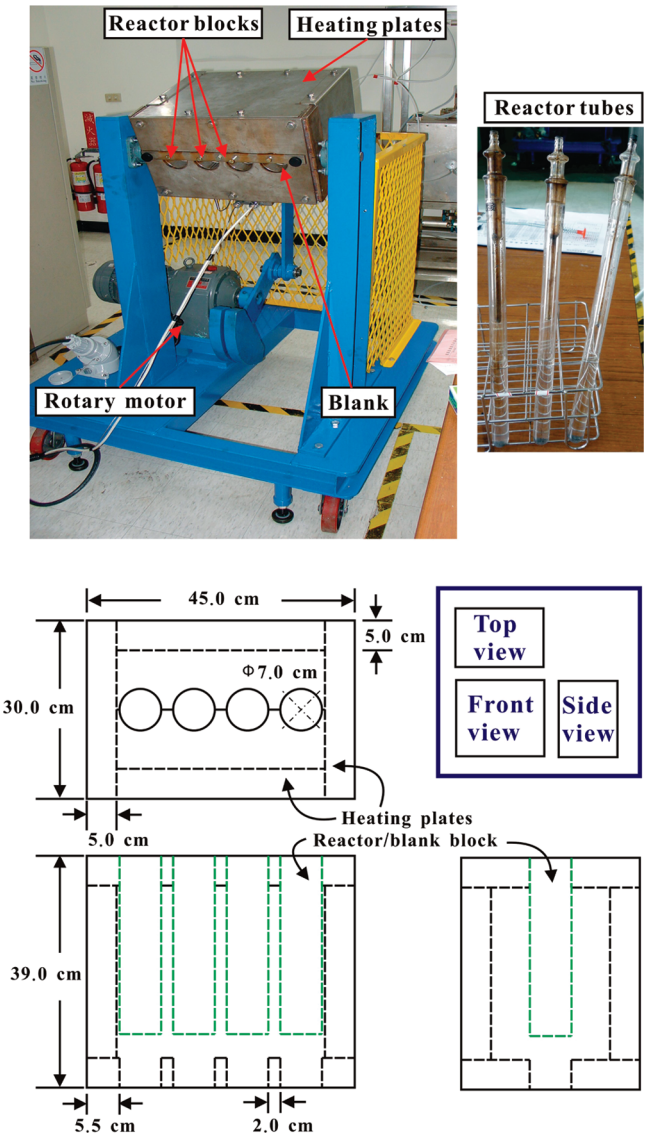

Figure 1. Photographs and diagram of the high-throughput system.

2.3. Activity Testing. An in-house designed batch-type high-throughput system (Figure 1) was employed in catalytic HDO testing. This system consisted of four heating plates, three reactor blocks, and a blank block. The heating plates were placed around the reactor and blank blocks with electric heating control. The reactor and blank blocks were aligned in an array. Three Pyrex reactor tubes measuring 25.0 cm long and 1.6 cm wide (30.0 mL, Figure 1) served as containers for the reactant, solvent, and catalyst. About 0.23 g of GUA and 7.63 g of tetradecane ($C_{14}H_{30}$) were employed to set the reactant-to-solvent ratio close to 3 wt %. A rotary motor was set at 100 rpm during the testing to ensure good mixing.

Approximately 0.3 g of catalyst, with particle sizes ranging from 40 to 80 mesh (0.37−0.18 mm), was used per trial. Catalyst pretreatment was conducted for both types of catalysts prior to each test. The noble metal catalyst was reduced in situ at 300 °C under 10 bar of H_2 pressure for 30 min. CoMo and NiMo catalysts were activated by a reduction−sulfidation system in a 5 vol % H_2S/H_2 (110 mL/min) stream. The activation procedure was performed from room temperature to 360 °C at a rate of 0.5 °C/min and held for 3 h. After cooling back to room temperature, the system was purged with N_2 for 30 min. Sulfided catalyst was immediately

dx.doi.org/10.1021/ef101521z |Energy Fuels 2011, 25, 890–896

Table 1. BET Surface Areas and Sulfur Loadings of the HDO Catalysts

	Rh	PtRh	PdRh	CoMo	NiMo
S_{BET} (m^2/g)	6.60	7.00	5.90	1.50	3.00
sulfur (wt%)	-	-	-	5.57	6.03

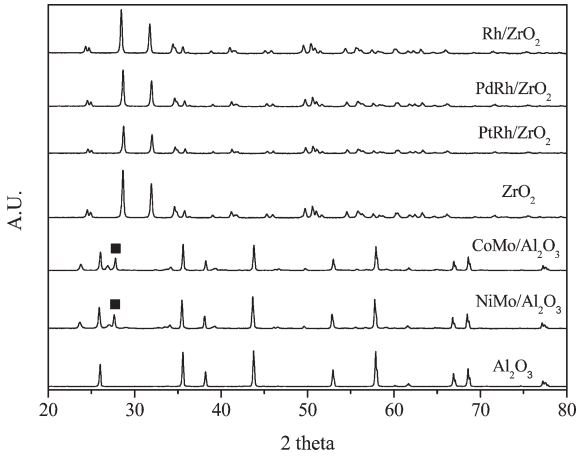

Figure 2. XRD patterns of the HDO catalysts.

transferred and mixed with reactant and solvent in the high-throughput system. The system was then flushed with N_2 (100 mL/min) for 30 min to evacuate air. All runs were operated under a hydrogen pressure of 50 bar. Two sets of comparative tests were performed: (1) at 400 °C for 20, 40, and 60 min, and (2) at 300, 350, and 400 °C for 60 min.

Identification of liquid products was conducted by a gas chromatograph−mass spectrometry system (GC/MS, Agilent 6890N and 5973N; with DB1701 capillary column); Quantitative analysis was performed with a GC/FID (Agilent 6890N) with the same column and programming as described above. Interpolated calibration was employed for product quantification using a standard solution of species. However, due to the lack of reference reagents, the calibrations of 2-methoxycyclohexanol ($C_7H_{14}O_2$) and 2-methoxycyclohexanone ($C_7H_{12}O_2$) were assumed to be the same FID response as 2-methylcyclohexanone ($C_7H_{12}O$), methoxybenzene (C_7H_8O) and methylphenol (C_7H_8O) were assumed to be equal to GUA, and cyclohexene (C_6H_{10}) was set equal to cyclohexanone ($C_6H_{10}O$).

The amount of coke was measured by a thermal gravimetric analyzer (TGA, Perkin-Elmer Pyris 1). The used catalyst was first purged with a N_2 stream at 280 °C for 1 h, followed by changing the sweeper gas to air at 600 °C (10 °C/min). Gaseous products were not collected due to the high-pressure batch-type design. The conversion of GUA (X), carbon yield of product (Y), and selectivity (S) were defined as follows:

$$X = \frac{(\text{moles of GUA})_{in} - (\text{moles of GUA})_{out}}{(\text{moles of GUA})_{in}} * 100\% \quad (1)$$

$$Y_i = \frac{\text{moles of carbon in product } i}{\text{moles of carbon in GUA}} * 100\% \quad (2)$$

$$S_i = \frac{\text{moles of carbon in product } i}{\text{the sum of carbon moles in products}} * 100\% \quad (3)$$

3. RESULTS AND DISCUSSION

3.1. Catalyst Characterization. Table 1 presents the surface areas of the catalysts used in this study. Slight differences were

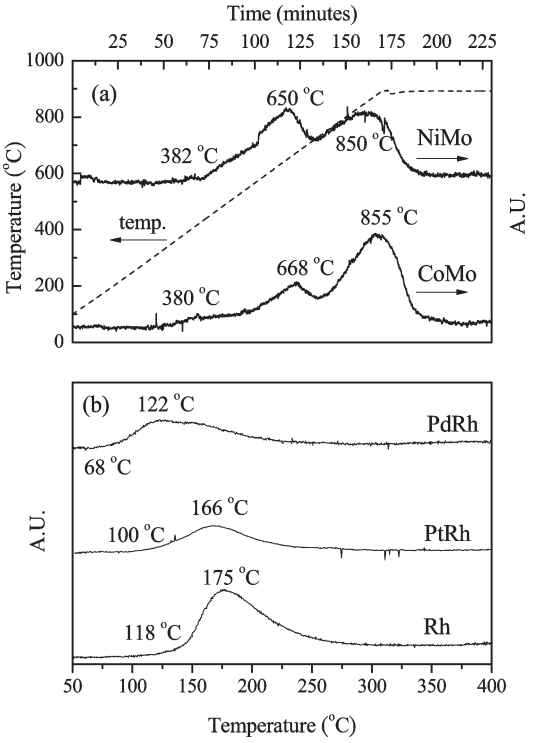

Figure 3. Temperature programmed reduction of (a) CoMo and NiMo/Al_2O_3 and (b) Rh-based catalysts.

observed, ranging from 1.5 to 7.0 m^2/g. Noble metal catalysts generally had larger surface areas than CoMo and NiMo catalysts. The sulfur loadings on sulfided CoMo/Al_2O_3 and NiMo/Al_2O_3 were 5.57 and 6.03 wt %, respectively. This is very similar to the work of Centeno and associates,[25] who showed the sulfur concentration on sulfided CoMo/Al_2O_3 was about 5.69 wt %. Figure 2 shows the XRD patterns of both noble metal and CoMo and NiMo catalysts. The XRD responses of noble metal catalysts were identical to that of the ZrO_2 support. This might be attributed to well-dispersed metal particles on the catalyst surface or a low level of metal loading, which was beyond the detection limit of XRD analysis. CoMo and NiMo catalysts exhibited a clear peak at 2θ = ~27°, indicating presence of $CoMoO_4$[34] and $NiMoO_4$.[35]

Figure 3 shows the H_2-TPR profiles. The onset (T_i) and maximum reduction (T_{max}) temperatures are also indicated in Figure 3. For Rh-based catalysts, the descending order of T_i and T_{max} was Rh > PtRh > PdRh. The reduction profiles exhibited significantly different shapes: the bimetallic catalysts had broader peaks than the Rh catalyst. This suggests the chemical interactions between the metals in bimetallic catalyst. Moreover, bimetallic PdRh and PtRh could be more reducible than the monometallic Rh catalyst.[32] CoMo and NiMo catalysts exhibited two major peaks in TPR. The first appeared at 650−670 °C, while the second appeared at approximately 850 °C. This is in agreement with earlier studies, which correlate the first peak to a partial reduction of Mo ions (Mo^{6+} to Mo^{4+}) and the second peak to deep reduction.[36−38] The influence of Co on CoMo or Ni on NiMo was insignificant in varying the TPR profiles.[36]

Figure 4 displays the GUA TPD patterns. Although it is very difficult to interpret TPD profiles with certainty,[39] a comparative study can approximate the strength of chemisorbed GUA. Results showed that both Al_2O_3 and ZrO_2 can chemisorb

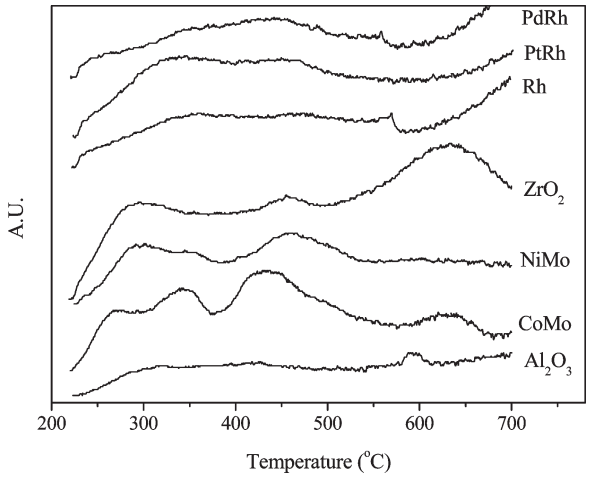

Figure 4. Temperature programmed desorption of GUA.

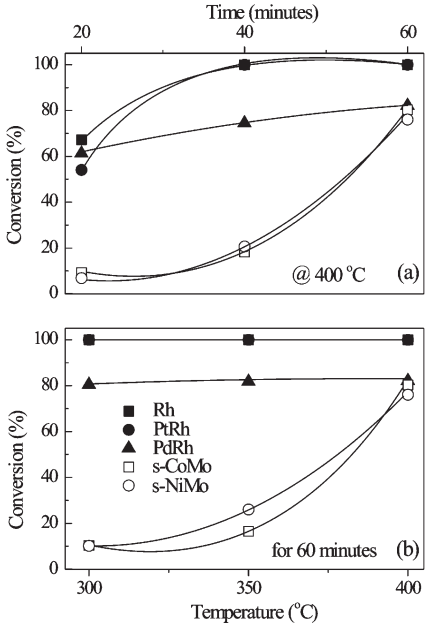

Figure 5. GUA conversion over Rh-based catalysts and sulfided CoMo and NiMo/Al_2O_3 as a function of (a) reaction time and (b) temperature.

GUA molecules. While Al_2O_3 showed no significant response, ZrO_2 exhibited at least three peaks. In addition, the area of the TPD peaks of ZrO_2 was greater than that of Al_2O_3, suggesting species could be released from the ZrO_2 surface more easily than from Al_2O_3 due to a weaker bond. This result agrees with Popov and co-workers,[40] who studied GUA adsorption on oxides (SiO_2, Al_2O_3, and $SiO_2-Al_2O_3$) with different acid−base properties. In their work, GUA interacted strongly with acidic Al_2O_3 in the form of doubly anchored phenates, a potential coke precursor. Decreasing the oxide's acidity suppresses the amount of doubly anchored phenates.[40] Upon incorporating an active phase, CoMo or NiMo/Al_2O_3 displayed newly formed peaks (at ~250, 350, and 450 °C). This implies the presence of potential active sites for GUA HDO. Rh-based catalysts exhibited two weak responses at approximately 300−350 °C and 400−500 °C. Gradually increasing signals appeared after elevating the temperature to 600 °C and above. Disparate HDO chemistry was

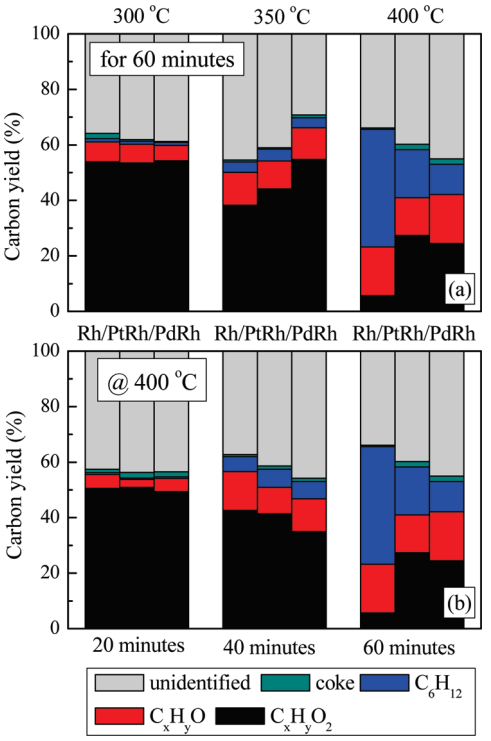

Figure 6. Carbon yields for GUA HDO with Rh-based catalysts. Reaction conditions: (a) H_2-pressure 50 bar, reaction time 60 min; (b) H_2-pressure 50 bar, reaction temperature 400 °C. Key: unidentified: gray; coke: cyan; cyclohexane: blue; 1-oxygen containing oxygenates ($C_7H_{14}O$, $C_6H_{12}O$, and $C_6H_{10}O$): red; and 2-oxygen containing oxygenates ($C_7H_{14}O_2$ and $C_7H_{12}O_2$): black.

expected because these two types of catalysts showed different results in GUA TPD.

3.2. Reactivity. Prior to the experiments, blank runs without catalyst and effects of supports (ZrO_2 and Al_2O_3 used as catalysts) were surveyed. These trials showed negligible influences for homogeneous reaction and supports. Figure 5a displays GUA conversion as a function of reaction time at 400 °C. Noble metal catalysts were very active. More than 50% conversion was achieved at 20 min after starting the reaction. The trend then leveled off (100% conversion) after 40−60 min. Sulfided CoMo and NiMo catalysts were less reactive than the noble metals from 20 to 60 min, and only converted a significant amount of GUA at 60 min after start-up (~80%). Figure 5b shows GUA conversion as a function of temperature for a 60-min reaction period. Rh and PtRh displayed full conversion, while PdRh had ~80%. Sulfided CoMo and NiMo exhibited significant GUA conversion at 400 °C. Clearly, Rh-based catalysts are more active than sulfided CoMo and NiMo.

The experiments in this study identified eleven major species. Rh-based catalysts produced 2-methoxycyclohexanol, 2-methoxycyclohexanone, 1-methoxycyclohexane ($C_7H_{14}O$), cyclohexanol ($C_6H_{12}O$), and cyclohexanone. Sulfided CoMo and NiMo produced methoxybenzene, methylphenol, phenol (C_6H_6O), benzene (C_6H_6), and cyclohexene. Both systems yielded cyclohexane (C_6H_{12}). Figure 6 shows the carbon yields of Rh-based catalysts for GUA HDO. Due to the lack of a mass spectrum database for 2-methoxycyclohexanol, the spectrum of 4-methoxycyclohexanol ($C_7H_{14}O_2$) from NIST Chemistry WebBook was used as a reference.[41] The electron ionization spectrum of

dx.doi.org/10.1021/ef101521z |*Energy Fuels* 2011, 25, 890–896

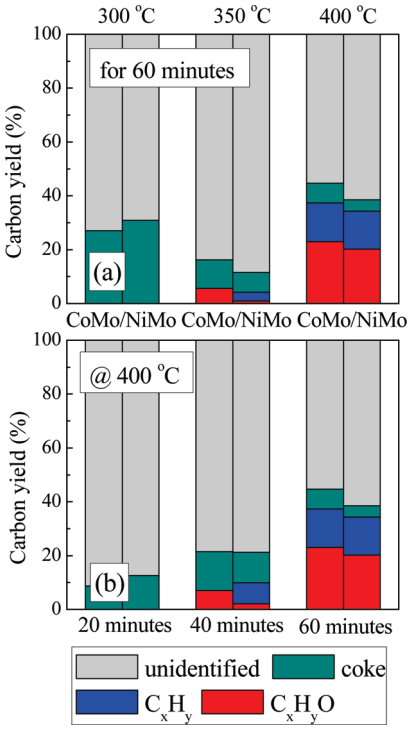

Figure 7. Carbon yields for GUA HDO with sulfided CoMo and NiMo catalysts. Reaction conditions: (a) H_2-pressure 50 bar, reaction time 60 min; (b) H_2-pressure 50 bar, reaction temperature 400 °C. Key: unidentified: gray; coke: cyan; hydrocarbons (C_6H_6, C_6H_{10}, and C_6H_{12}): blue; 1-oxygen containing oxygenates (C_6H_6O and C_7H_8O): red.

4-methoxycyclohexanol is very similar to the speculated product, i.e., 2-methoxycyclohexanol, showing the strongest ion fragments at m/z = 72, 71, and 73. Therefore, it is highly plausible that this product is 2-methoxycyclohexanol.

The yields of two oxygen-containing products decreased with increasing temperature, while cyclohexane increased. Among the Rh-based catalysts, the monometallic Rh catalyst generated the highest yield of cyclohexane (~42%) in the final stage. Moreover, the mono-oxygen compounds had the highest yield. The same trend appeared by illustrating carbon yields as a function of reaction time. This indicates that the monometallic Rh catalyst possessed the highest HDO reactivity of the Rh-based catalysts. However, H_2-TPR revealed that it is less reducible than bimetallic PdRh and PtRh catalysts.

Figure 7 displays the carbon yield of GUA HDO by sulfided CoMo and NiMo as a function of reaction temperature and time. No products except coke could be identified under 300 °C for 60 min and 400 °C for 20 min. This might be attributed to low conversions of GUA (15% and less), at which GUA transformation was at its initial stage, yielding an insignificant amount of products.[31,43,42] As temperature and time increased, product yields increased and coke formation decreased. The main products were (1) mono-oxygen containing species including methoxybenzene, methylphenol, and phenol, and (2) hydrocarbons including benzene, cyclohexene, and cyclohexane. The two-oxygen containing compounds generated by noble metal catalysts were absent. Note that the unidentified species might include methane, methanol, and heavier products like cyclohexylbenzene and methylcyclopentane. These compounds were reported to be the major byproducts of GUA HDO.[25,31,43,42]

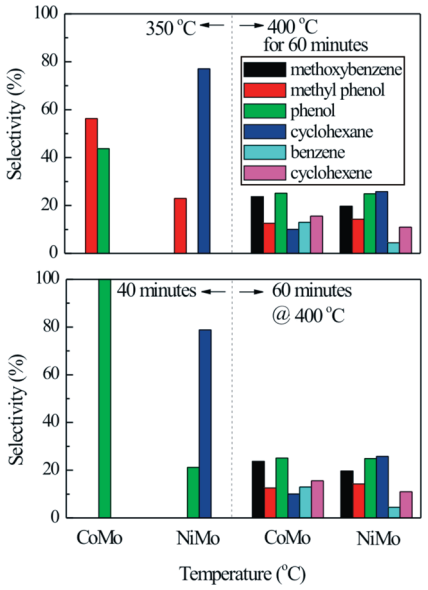

Figure 8. Product selectivity of sulfided CoMo and NiMo catalysts.

Figure 8 presents a detailed examination of the product selectivity. It is worth noting that selectivity of cyclohexane was significantly high (~80%) for NiMo catalyst under 40 min at 400 °C and 60 min at 350 °C, whereas phenol and methylphenol were the main products for CoMo. This implies that sulfided NiMo had a stronger influence on benzene ring hydrogenation than that of sulfided CoMo. More coke was formed on sulfided CoMo and NiMo catalysts than the noble metals. This might be attributed to the coke precursors, e.g., catechol ($C_6H_6O_2$), formed by the CoMo and NiMo catalysts.[13,44]

Sulfur stripping from catalyst surface was observed for all trials using sulfided catalysts. With increasing experimental severity, the sulfur contents in liquid samples increased from 0.03 to 0.44 wt % for $CoMo/Al_2O_3$ and 0.03 to 0.15 wt % for $NiMo/Al_2O_3$. As reported by Gutierrez and associates, the yielded sulfur-containing species during GUA HDO could be methanethiol, dimethyl sulfide, cyclohexanethiol, and methylthiocyclohexane.[32]

3.3. Mechanism. Figure 9 shows the proposed GUA HDO mechanisms for the two types of catalysts in this study. The first step for Rh-based catalysts was hydrogenation of GUA's benzene ring, yielding 2-methoxycyclohexanol and 2-methoxycyclohexanone as the major products. The second step was demethoxylation and dehydoxylation to form cyclohexane as the final product. As for sulfided CoMo and NiMo catalysts, GUA HDO proceeded through demethylation, demethoxylation, and deoxygenation. Early studies suggested that demethylation, which produced catechol through hydrogenolysis of the methyl-oxygen bond, was the onset of GUA HDO.[21−24] Later, considerable amount of phenol was discovered at the initial stage of GUA HDO,[25,29] implying hydrogenolysis of the aromatic carbon−oxygen bond, i.e., demethoxylation. This was confirmed by Bui and co-workers[43,42] who identified both phenol and methanol at the initial stage using sulfided CoMo catalysts. Therefore, it is highly plausible that demethylation, demethoxylation, and deoxygenation proceed concurrently in the proposed system. The mono-oxygenates, including phenol, methoxybenzene, and methyl phenol, were subsequently converted to form benzene. In a hydrogen-rich environment, benzene double bonds can be partially or fully saturated to form cyclohexene and cyclohexane. Note that catechol was not observed. A possible explanation might

dx.doi.org/10.1021/ef101521z |*Energy Fuels* 2011, 25, 890–896

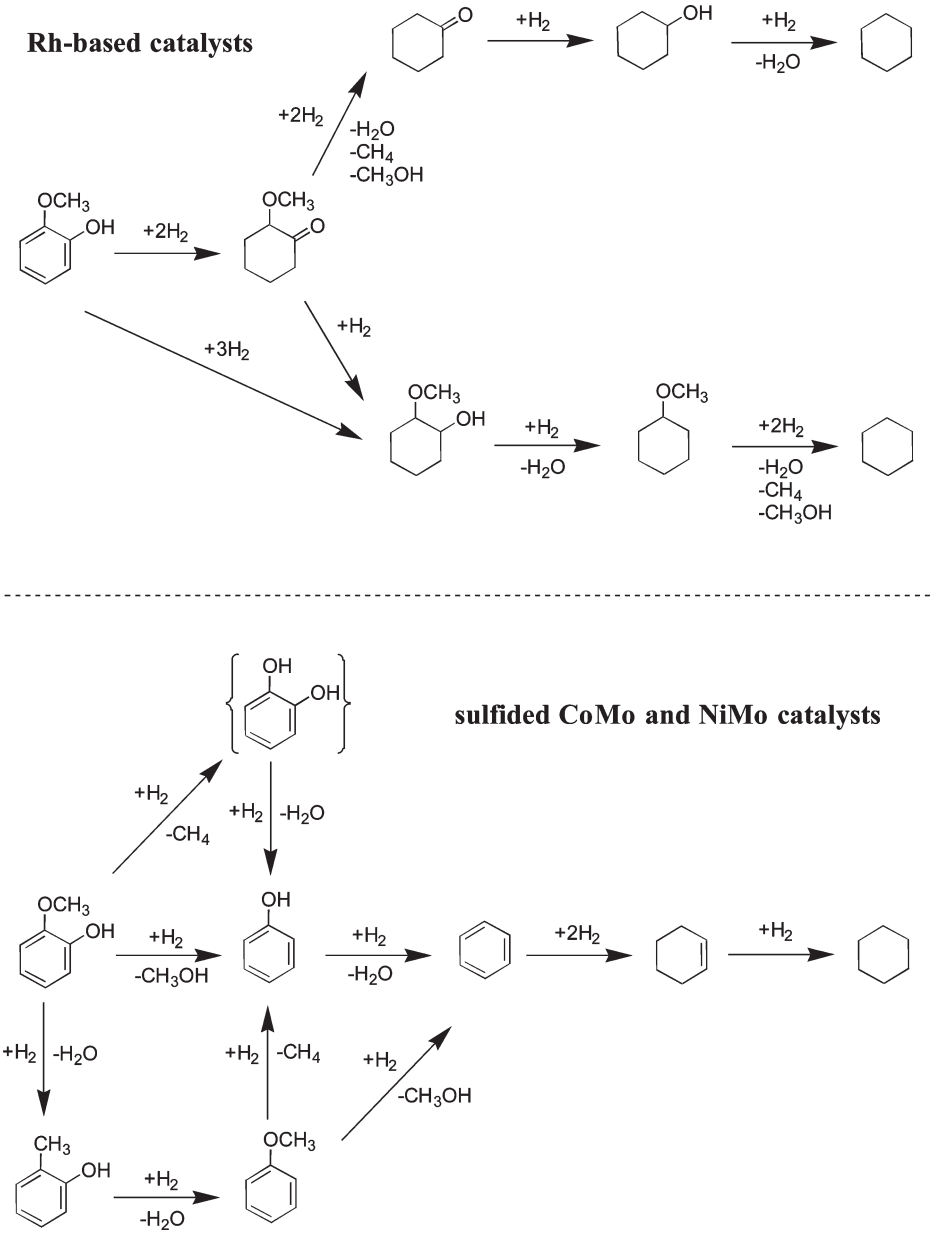

Figure 9. Mechanism of GUA HDO by Rh-based and sulfided CoMo and NiMo catalysts.

be that catechol was converted during the sampling period or handling process. This was confirmed by the significant amount of coke[13] observed at initial conditions (300 °C, 60 min and 400 °C, 20 min). Zhao and co-workers reported similar behavior using transition metal phosphides in gas phase GUA HDO in a continuous fixed bed system.[44] No catechol could be observed after longer contact times.

4. CONCLUSIONS

The Rh-based and sulfided CoMo and NiMo catalysts in this study exhibited significantly different catalytic behaviors in GUA HDO. Monometallic or bimetallic Rh catalysts showed greater activity than CoMo and NiMo. Bimetallic catalysts produced no noticeable improvement. Instead, the PdRh catalyst had some adverse effects on activity. The activity of both sulfided CoMo and NiMo was almost identical. Rh/ZrO_2 was the most effective among the noble metal catalysts, yielding the most cyclohexane after 1 h at 400 °C. Product analysis suggests that the mechanism of GUA HDO promoted by Rh-based catalysts involved two consecutive steps: hydrogenation of the GUA benzene ring, followed by demethoxylation and dehydoxylation of oxygenates. For sulfided CoMo and $NiMo/Al_2O_3$, the HDO process began with demethylation, demethoxylation, and deoxygenation, followed by benzene ring saturation. This explains the difference in product distributions of these catalysts.

In summary, the Rh-based catalyst exhibited the best HDO activity, but tended to saturate valuable benzene rings. Classical sulfided CoMo and NiMo catalysts showed potential in making aromatics, but were relatively inert compared to noble metals and produced significant coke. Future advances in understanding HDO surface chemistry both experimentally and theoretically should allow researchers to design improved catalysts to produce targeted products from lignin and its derivatives.[45,46]

AUTHOR INFORMATION

Corresponding Author
*E-mail: yclin@saturn.yzu.edu.tw.

ACKNOWLEDGMENT

Valuable suggestions of Prof. Geoff A. Tompsett (University of Massachusetts-Amherst) and anonymous reviewers are gratefully appreciated. The authors also acknowledge financial support provided by the Bureau of Energy, Ministry of Economics Affairs, Taiwan (99-D0103).

REFERENCES

(1) Crawford, R. L. *Lignin Biodegradation and Transformation*; Wiley-Interscience: New York, 1981.
(2) Holladay, J. E.; White, J. F.; Bozell, J. J.; Johnson, D. *Top Value-Added Chemicals from Biomass; Volume II, Results of Screening for Potential Candidates from Biorefinery Lignin*; PNNL-16983; Pacific Northwest National Laboratory: Richland, WA, 2007.
(3) Struszczyk, H. In *Lignin: Properties and Materials*; Glasser, W. G., Sarkanen, S., Eds.; American Chemical Society: Washington, DC, 1989; p 245.
(4) Gosselink, R. J. A.; de Jong, E.; Guran, B.; Abacherli, A. *Ind. Crops Prod.* **2004**, *20*, 121–129.
(5) Zakzeski, J.; Bruijnincx, P. C. A.; Jongerius, A. L.; Weckhuysen, B. M. *Chem. Rev.* **2010**, *110*, 3552–3599.
(6) Huber, G. W. *Breaking the Chemical and Engineering Barriers to Lignocellulosic Biofuels: Next Generation Hydrocarbon Biorefineries*; University of Massachusetts-Amherst, 2008.
(7) Mohan, D.; Pittman, C. U.; Steele, P. H. *Energy Fuels* **2006**, *20*, 848–889.
(8) Huber, G. W.; Iborra, S.; Corma, A. *Chem. Rev.* **2006**, *106*, 4044–4098.
(9) Sealock, L. J.; Elliott, D. C.; Baker, E. G.; Butner, R. S. *Ind. Eng. Chem. Res.* **1993**, *32*, 1535–1541.
(10) Elliott, D. C.; Hart, T. R. *Energy Fuels* **2009**, *23*, 631–637.
(11) Chheda, J. N.; Huber, G. W.; Dumesic, J. A. *Angew. Chem., Int. Ed.* **2007**, *46*, 7164–7183.
(12) Li, N.; Huber, G. W. *J. Catal.* **2010**, *270*, 48–59.
(13) Furimsky, E. *Appl. Catal., A* **2000**, *199*, 147–190.
(14) Dorrestijn, E.; Laarhoven, L. J. J.; Arends, I. W. C. E.; Mulder, P. *J. Anal. Appl. Pyrolysis* **2000**, *54*, 153–192.
(15) Pattiya, A.; Titiloye, J. O.; Bridgwater, A. V. *J. Anal. Appl. Pyrolysis* **2008**, *81*, 72–79.
(16) Kleinert, M.; Barth, T. *Energy Fuels* **2008**, *22*, 1371–1379.
(17) Klein, M. T.; Virk, P. S. *Energy Fuels* **2008**, *22*, 2175–2182.
(18) Hou, Z.; Bennett, C. A.; Klein, M. T.; Virk, P. S. *Energy Fuels* **2010**, *24*, 58–67.
(19) Binder, J. B.; Gray, M. J.; White, J. F.; Zhang, Z. C.; Holladay, J. E. *Biomass Bioenergy* **2009**, *33*, 1122–1130.
(20) Alpert, S. B.; Shuman, S. C. Canadian Patent 851709, 1970.
(21) Hurff, S. J.; Klein, M. T. *Ind. Eng. Chem. Fundam.* **1983**, *22*, 426–430.
(22) Kallury, R. K. M. R.; Restivo, W. M.; Tidwell, T. T.; Boocock, D. G. B.; Crimi, A.; Douglas, J. *J. Catal.* **1985**, *96*, 535–543.
(23) Bredenberg, J. B.-S.; Huuska, M.; Toropainen, P. *J. Catal.* **1989**, *120*, 401–408.
(24) Laurent, E.; Delmon, B. *Appl. Catal., A* **1994**, *109*, 77–96.
(25) Centeno, A.; Laurent, E.; Delmon, B. *J. Catal.* **1995**, *154*, 288–298.
(26) Ferrari, M.; Maggi, R.; Delmon, B.; Grange, P. *J. Catal.* **2001**, *198*, 47–55.
(27) Ferrari, M.; Delmon, B.; Grange, P. *Carbon* **2002**, *40*, 497–511.
(28) Ferrari, M.; Delmon, B.; Grange, P. *Microporous Mesoporous Mater.* **2002**, *56*, 279–290.
(29) de la Puente, G.; Gil, A.; Pis, J. J.; Grange, P. *Langmuir* **1999**, *15*, 5800–5806.
(30) Pinheiro, A.; Hudebine, D.; Dupassieux, N.; Geantet, C. *Energy Fuels* **2009**, *23*, 1007–1014.
(31) Bui, V. N.; Toussaint, G.; Laurenti, D.; Mirodatos, C.; Geantet, C. *Catal. Today* **2009**, *143*, 172–178.
(32) Gutierrez, A.; Kaila, R. K.; Honkela, M. L.; Slioor, R.; Krause, A. O. I. *Catal. Today* **2009**, *147*, 239–246.
(33) Li, C.-L.; Lin, Y.-C. *Catal. Lett.* **2010**, *140*, 69–76.
(34) Hada, K.; Tanabe, J.; Omi, S.; Nagai, M. *J. Catal.* **2002**, *207*, 10–22.
(35) Brito, J. L.; Laine, J. *J. Catal.* **1993**, *139*, 540–550.
(36) Arnoldy, P.; Franken, M. C.; Scheffer, B.; Moulijn, J. A. *J. Catal.* **1985**, *96*, 381–395.
(37) Qu, L.; Zhang, W.; Kooyman, P. J.; Prins, R. *J. Catal.* **2003**, *215*, 7–13.
(38) El Kady, F. Y. A.; Abd El Wahed, M. G.; Shaban, S.; Abo El Naga, A. O. *Fuel* **2010**, *89*, 3193–3206.
(39) Gorte, R. J. *Catal. Today* **1996**, *28*, 405–414.
(40) Popov, A.; Kondratieva, E.; Goupil, J. M.; Mariey, L.; Bazin, P.; Gilson, J.-P.; Travert, A.; Mauge, F. *J. Phys. Chem. C* **2010**, *114*, 15661–15670.
(41) *NIST Chemistry WebBook*; National Institute of Standards and Technology: Gaithersburg, MD, 2005.
(42) Bui, V. N.; Laurenti, D.; Afanasiev, P.; Geantet, C. *Appl. Catal., B* **2010**, *101*, 239–255.
(43) Bui, V. N.; Laurenti, D.; Delichere, P.; Geantet, C. *Appl. Catal., B* **2010**, *101*, 246–255.
(44) Zhao, H. Y.; Li, D.; Bui, P.; Oyama, S. T. *Appl. Catal., A* **2010**, *391*, 305–310.
(45) Lin, Y.-C.; Huber, G. W. *Energy Environ. Sci.* **2009**, *2*, 68–80.
(46) Vlachos, D. G.; Caratzoulas, S. *Chem. Eng. Sci.* **2010**, *65*, 18–29.